# ELASTIC ELECTRON SCATTERING OFF $^3$He AND $^4$He AT LARGE MOMENTUM TRANSFERS

Jefferson Lab PAC18 Proposal, July 2000


K. A. Aniol, M. B. Epstein, D. J. Margaziotis

*California State University, Los Angeles, CA 90032*

P. E. C. Markowitz

*Florida International University, Miami, FL 33199*

J. A. Templon

*University of Georgia, Athens, GA 30602*

R. De Leo

*INFN/Bari and University of Bari, 70126 Bari, Italy*

E. Cisbani, S. Frullani, F. Garibaldi, M. Iodice, R. Iommi, G. M. Urciuoli

*INFN/Sanità and ISS Physics Lab., 00161 Rome, Italy*

J.-P. Chen, J. Gomez, C. W. de Jager, M. Kuss, N. Liyanage, J. J. LeRose

*Jefferson Lab, Newport News, VA 23606*

B. D. Anderson, A. T. Katramatou, D. M. Manley, G. G. Petratos, J. W. Watson, W.-M. Zang

*Kent State University, Kent, OH 44242*

E. J. Beise, C.-C. Chang

*University of Maryland, College Park, MD 20742*

A. Hotta, K. S. Kumar, G. A. Peterson, S. E. Rock
*University of Massachusetts, Amherst, MA 01003*

W. Bertozzi, S. Gilad, D. W. Higinbotham, R. Suleiman
*Massachusetts Institute of Technology, Cambridge, MA 02139*

J. R. Calarco
*University of New Hampshire, Durham, NH 03824*

L. E. Marcucci
*Old Dominion University, Norfolk, VA 23529*

T. Suda
*RIKEN, Institute of Physical and Chemical Research, Saitama 351, Japan*

S. Dieterich, R. Gilman, C. Glashausser, X. Jiang, G. Kumbartzki, R. D. Ransome, S. Strauch
*Rutgers, The State University of New Jersey, Piscataway, NJ 08855*

M. N. Olson
*St. Norbert College, De Pere, WI 54115*

L. Auerbach, S. Choi, Z.-E. Meziani
*Temple University, Philadelphia, PA 19122*

K. Kino and T. Tamae
*Tohoku University, Laboratory of Nuclear Science, Sendai 982, Japan*

Spokespersons: J. Gomez and G. G. Petratos

## ABSTRACT

We repropose to measure elastic electron scattering off the $^3$He and $^4$He few-body systems up to the highest momentum transfers possible, limited by cross section sensitivity. The original proposal, E89-21, was approved in 1989 for one month of beam time. The measurements will extend our knowledge of the elastic form factors of the helium isotopes down by more than one order in magnitude and out in $Q^2$ possibly by more than a factor of two. The experiment will use the Hall A Facility of JLab. Scattered electrons will be detected in the Electron High Resolution Spectrometer. Recoil nuclei will be detected in coincidence with the scattered electrons in the Hadron High Resolution Spectrometer. The results are expected to play a crucial role in establishing the standard model describing the structure of few-body nuclei in terms of nucleons and mesons and possibly providing evidence for its break-down at "large" momentum transfers, where the quark-gluon degrees of freedom are expected to dominate. We request 45 days of beam time at a beam current of 100 $\mu$A for helium production data and hydrogen calibrations.

# 1 Motivation

The electromagnetic form factors of the $^3$He and $^4$He isotopes provide the most detailed information on their wave functions. The wave functions are very sensitive to the choice of the nucleon-nucleon interaction, the treatment of meson-exchange currents and relativistic corrections, and to a possible admixture of multi-quark states. The few-body factors, along with the deuteron elastic structure functions are the "observables of choice" [1] for testing the nucleon-meson standard model [2] of the nuclear interaction and the associated current operator. At large momentum transfers they may offer a unique opportunity to uncover a possible transition from the meson-nucleon to quark-gluon degrees of freedom as predicted by quark dimensional-scaling [3].

Experimentally, the $^3$He and $^4$He charge, $F_C$, and magnetic, $F_M$, form factors are determined from elastic electron scattering studies. The cross section for elastic electron scattering from the spin 1/2 $^3$He nucleus is given by:

$$\frac{d\sigma}{d\Omega} = \frac{(Z\alpha)^2 E'}{4E^3 \sin^4\left(\frac{\Theta}{2}\right)} \left[ A(Q^2)\cos^2\left(\frac{\Theta}{2}\right) + B(Q^2)\sin^2\left(\frac{\Theta}{2}\right)\right]$$

where $\alpha$ is the fine-structure constant, $Z$ is the nuclear charge, $E$ and $E'$ are the incident and scattered electron energies, $\Theta$ is the electron scattering angle, $Q^2 = 4EE'\sin^2(\Theta/2)$ is the squared four-momentum transfer, and $A(Q^2)$ and $B(Q^2)$ are the elastic structure functions:

$$A(Q^2) = \frac{F_C^2(Q^2) + \mu^2\tau F_M^2(Q^2)}{1+\tau},$$

$$B(Q^2) = 2\tau\mu^2 F_M^2(Q^2),$$

where $\tau = Q^2/4M^2$, and $\mu$ and $M$ are the magnetic moment and mass of the target nucleus. The two form factors of $^3$He are determined by measuring the elastic cross section at several angles for the same $Q^2$ (Rosenbluth separation). The cross section for elastic electron scattering from the spin 0 $^4$He nucleus is given by:

$$\frac{d\sigma}{d\Omega} = \frac{(Z\alpha)^2 E' \cos^2\left(\frac{\Theta}{2}\right)}{4E^3 \sin^4\left(\frac{\Theta}{2}\right)} F_C^2(Q^2).$$

The $^4$He charge form factor is determined by forward angle cross section measurements.

Theoretically, the $^3$He and $^4$He form factors are calculated using numerical solutions of the Faddeev equations, the correlated hyperspherical harmonics (CHH) variational method, or Monte Carlo methods to solve for the nuclear ground states. All three methods provide a solution of the Schrödinger equation for non-relativistic nucleons bound by the nucleon-nucleon interaction. The Faddeev decomposition for the three- or four-body problem rewrites the Schrödinger equation as a sum of three or four equations, in which only one pair of nucleons (for two-nucleon interactions, at least) interacts at a time . The resulting equations are solved in either momentum [4, 5] or coordinate [6, 7] space. The CHH variational method [1] is based on a decomposition quite similar to the Faddeev one. The primary differences are the introduction of hyperspherical coordinates and inclusion of the strong state-dependent correlations, induced by the nucleon-nucleon interaction, directly in the definition of the nuclear wave function. The principal Monte Carlo schemes developed are variational and Green's function Monte Carlo. Variational Monte Carlo (VMC) [8, 9, 10, 11] uses Monte Carlo techniques to perform standard numerical quadratures. Green's function Monte Carlo (GFMC) [10, 12] employs Monte Carlo methods to evaluate the imaginary-time path integrals relevant for a light nucleus.

The simple description of light nuclei based on a non-relativistic many-body theory, where the nuclear electromagnetic operators are expressed in terms of those associated with the individual protons or neutrons [impulse approximation (IA), see Fig. 1a] is incomplete. Meson-exchange mechanisms [13] naturally lead to effective many-body current operators. The investigation of meson-exchange current (MEC) effects on the electromagnetic form factors of the deuteron and few-body nuclei has conclusively proven that a satisfactory qualitative description of these form factors requires a current operator that includes two-body components.

The two-body currents fall into two categories. In the first category are those constrained by the continuity equation and directly determined from the nucleon-nucleon interaction (isovector currents associated with pion-like exchanges, see Figs. 1b and 1c). Since they do not contain any free parameters, they are viewed as "model-independent". The currents in the second category are "model-dependent" and are associated with electromagnetic transition couplings between different mesons (isoscalar $\rho\gamma\pi$ and isovector $\omega\gamma\pi$ transition

currents, see Fig. 1d), or with excitation of intermediate nucleon resonances, specifically the $\Delta$-isobar (see Fig. 1e).

The introduction of isobar configurations in the description of the few-body systems is accomplished by approximate perturbative techniques [13], by solving the coupled-channel Schrödinger equation [14], or by a generalization of the correlation operator technique [15] in the context of variational methods. Isobar configurations have only small effects on the calculated few-body form factors [1].

The question whether "three-body force" effects [16] by three-body interactions (see Figs. 1f and 1g) influence the trinucleon form factors has been examined by Friar and collaborators [17] and more recently by Marcucci and collaborators [1]. The former (latter) study has shown that the effect of the three-nucleon interaction on the charge (magnetic) $^3$He form factor is small. A similar conclusion has been drawn by Katayama and collaborators [18] for the charge form factor of $^4$He.

An important question is whether mesonic and nucleonic degrees of freedom are sufficient for a quantitative understanding of the three- and four-body systems at large momentum transfers, where the nucleonic substructure and dynamics are generally recognized to make an increasing contribution and probably dominate. In an attempt to simultaneously incorporate the quark- and gluon-exchange mechanism at short-distance and the meson-exchange mechanism at long- and intermediate-distance, several groups [19, 20, 21, 22, 23] have developed composite meson-nucleon and multi-quark superposition approaches in the calculation of the $^3$He and $^4$He form factors.

Typical models, which incorporate both nucleonic-mesonic and quark degrees of freedom are a) a hybrid quark-hadron model [22] in which the main parameter is the separation $r_\circ \sim 1$ fm between the "internal" quark cluster region of overlapping nucleons and the "external" hadronic region, where the nucleons have little overlap and solutions to the Faddeev equations are used, and b) a multiple-quark compound model based on the relativistic harmonic oscillator quark model [21]. The hybrid models are in general able to reproduce the existing data but are still in a phenomenological stage and with sufficient freedom in the choice of elementary parameters used. The hope is that the hybrid models could provide a basis for a quantitative description of the short-distance quark structure of the few-body

systems and a bridge for treating short-range phenomena with a more fundamental quantum chromodynamics prescription.

Another approach trying to incorporate the quark-gluon substructure of the helium isotopes is, as for the deuteron case, the dimensional-scaling quark model [24]. The principal ideas of this model are dimensional scaling of high energy amplitudes using quark counting, leading to a) the prediction for the "helium form factor" $F_{\rm He}(Q^2) \equiv \sqrt{A(Q^2)}$ that $F_{\rm He} \sim (Q^2)^{1-3A}$, where $A = 3$ (4) for $^3$He ($^4$He), respectively, and b) the dominance of the constituent-interchange force between quarks of different nucleons to share $Q/A$. The contention is that this quark-interchange model contains the important dynamics for the helium form factors at large $Q^2$ and is similar to, if not the same, as particular meson-exchange diagrams. The three relevant diagrams, a) democratic 9-quark chain model, b) nucleon-dinucleon quark interchange, and c) three-nucleon quark interchange are shown in Fig. 2. Similarly the $^4$He form factor can be described as a chain of twelve quarks or a skeletal four-nucleon structure, neutron-$^3$He or deuteron-deuteron with quark interchanges.

Figures 3 and 4 show experimental data for the $^3$He charge and magnetic form factors up to date from Stanford [25, 26], Orsay [27], Saclay [28, 29], Bates [30, 31], Mainz [32] and SLAC [33] experiments.[1] The data demonstrate the presence of an expected diffraction minimum for both form factors. They are compared to four "full" calculations by Hadjimichael and collaborators [7], Strueve and collaborators [5], Schiavilla and collaborators [8, 9] and Wiringa [10] (see below), that include, in addition to the impulse approximation, meson-exchange currents and genuine three-body force effects. The theoretical impulse approximation, not shown in the Figures, totally fails to describe the data. It grossly overestimates (underestimates) the location of the diffraction minimum and underestimates (overestimates) the secondary maximum of $F_C$ ($F_M$), necessitating the need for inclusion of meson-exchange currents. The above calculations describe fairly well the charge form factor data, but fail to reproduce the position of the magnetic form factor minimum. Some authors [34] have attributed this disagreement to the need for fully relativistic calculations [35, 36] for the three-body form factors. Figures 5 and 6 show the predictions of selected IA+MEC theoretical calculations at higher momentum transfers, accessible by JLab. All calculations predict

[1] Additional data are expected in the near future from a measurement of the $^3$He magnetic form factor at Bates.

the presence of a second diffraction minimum for the $^3$He form factors that can be observed at Jefferson Lab.

Figure 7 shows the available experimental data up to date for the $^4$He charge form factor from Stanford [26, 37], Mainz [32] and SLAC [33] measurements. The data, which clearly demonstrate the presence of a diffraction minimum at $\simeq$ 10 fm$^{-2}$, are compared to the impulse approximation and complete (IA+MEC) calculations by Wiringa [10] and Schiavilla and collaborators [9]. As in the case of $^3$He, the impulse approximation alone cannot describe the data, overestimating the location of the diffraction minimum and underestimating the height of the secondary maximum. Although the inclusion of meson-exchange currents brings the theory in fair agreement with the data, none of the full calculations can describe, at the same time, both the Stanford and SLAC data.

Hadjimichael and collaborators [7] solved the $^3$He coupled-channel Faddeev equations in coordinate space using several nucleon-nucleon potential models including the Paris and Reid Soft Core. The calculation included $\pi$, $\rho$, $\omega$, $\rho\gamma\pi$ and $\omega\gamma\pi$ meson-exchange currents plus isobar admixtures in the initial ground state wave function. Also included were the one-body Darwin-Foldy and spin-orbit relativistic corrections. Three-body force effects were accounted by including in the calculation the $2\pi$, $1\Delta$ three-body force term of Fig. 1g.

Strueve and collaborators [5] solved the $^3$He Faddeev equations in momentum space, and used the Paris nucleon-nucleon potential modified to include $\Delta$-isobar excitations via $\pi$ and $\rho$ meson-exchanges. The presence of the $\Delta$ thus accounted for the most important part of three-body force effects. The calculation included $\pi$, $\rho$, and $\rho\pi\gamma$ meson-exchange contributions as well as the above relativistic corrections.

Schiavilla and collaborators [8, 9] used variational three- and four-body wave functions computed with the Argonne $V_{14}$ potential and the Urbana-VII three-nucleon force model. In this calculation, the $\pi$-like and $\rho$-like meson-exchange currents were derived consistently from the nucleon-nucleon interaction used. The calculation included, in addition to the above relativistic corrections, contributions from $\omega$ and $\omega\gamma\rho$ meson-exchange currents.

Wiringa's calculations [10] for the $^3$He form factors were based on the same MEC model as to those of Schiavilla and collaborators and the Argonne $V_{14}$ potential. The $^3$He wave functions were determined with the Faddeev equations and three-body force effects were

accounted with the more recent Urbana-VIII three-nucleon force model. The $^4$He charge form factor was evaluated with a Monte Carlo variational wave function and a Green's function Monte Carlo wave function. The latter wave function is a $V_{14}$ potential upgraded calculation by Carlson [12].

**The objective of this proposal is to improve the quality of the existing data, where possible, and most importantly to extend the measurements of the $^3$He and $^4$He form factors to higher momentum transfers, where the standard meson-nucleon model predicts the presence of a second diffraction minimum in the kinematic regime accessible by the JLab Hall A Facility. The theoretical calculations are increasingly sensitive with $Q^2$ to the details of the nucleon-nucleon force and to the contributions of meson-exchange currents. Precision measurements of the helium form factors at large momentum transfers will be critical in establishing the parameters of the few-body standard model, testing our knowledge of the nucleon-nucleon potential, possible three-body force effects and the nature of meson-exchange currents. The measurements can also uncover a possible transition from the standard meson-nucleon model to a quark-gluon description, as predicted by quark dimensional-scaling, if it occurs in the four-momentum range accessible by this experiment. The luminosity of the experiment will be sufficient to discover the predicted second diffraction minima of the form factors or track an asymptotic fall-off in their absence.**

## 2 The Experiment

We propose to measure a) forward and backward elastic electron-$^3$He scattering, to separate the charge and magnetic form factors of $^3$He up to the maximum momentum transfer possible, and b) forward elastic electron scattering off $^4$He, to extract the charge form factor of $^4$He up to the maximum momentum transfer possible. The inelastic break-up threshold is 5.4 MeV for $^3$He and 20 MeV for $^4$He. For the $^3$He case, to ensure separation between elastic and inelastic scattering events, recoil nuclei will be detected in coincidence with the scattered electrons. The $^4$He measurements will rely on detection of only scattered electrons. As a

precaution, we plan to take simultaneously both single- and double-arm data. This strategy will allow us to cleanly identify, at the cost of a reduced solid angle, elastic events in the presence of unexpected single arm background.

The natural place to perform such measurements is the JLab Hall A Facility with its two large solid angle, high resolution spectrometers (HRS). Beam energies in the range of 0.5 to 1.4 GeV are required for the backward $^3$He measurements and 1.5 to 4.5 GeV for the forward $^3$He and $^4$He measurements. The scattered electron (recoil nucleus, $P_r$) momentum will be in the range of 0.4 to 4.0 (0.6 to 2.0) GeV/c. The electron scattering (recoil nucleus, $\Theta_r$) angle for the $^3$He backward data will be around 145° (14°), where the elastic cross section is dominated by the magnetic form factor (except around the $Q^2$ region of a diffraction minimum). The electron scattering (recoil nucleus) angle for the forward data will be around 20° (65°), for $^3$He, and 23° (around 70°) for $^4$He. An indicative detailed kinematic list is given, along with the ratio of the electron to recoil nucleus solid angle Jacobian, $(\Delta\Omega)_e/(\Delta\Omega)_r$, in Tables 1, 2 and 3.

The electron spectrometer will be used in its standard detector configuration of a drift chamber set, a gas threshold Čerenkov counter, a highly segmented preradiator/total absorption shower counter calorimeter, and two scintillation hodoscopes. The hadron spectrometer will require a subset of its detectors, namely the drift chamber set and the two scintillation hodoscopes. To minimize absorption of recoil nuclei, not-needed detectors will be pushed to the side as in the elastic electron-deuteron measurements of E91-26 [38]. To minimize the required beam time, we are proposing, as in the original proposal, to implement the large solid angle configuration of both HRS's, where the two first quadrupoles move closer to the target. The solid angle of this configuration is twice as large as the one of the standard configuration. The electron (hadron) HRS will be used in its large solid angle mode for the backward (forward) measurements.

The target system assumes three 20 cm long cells, two filled with 5 K/15 atm gas $^3$He and $^4$He and one filled with liquid hydrogen. These cells are currently under development. The $^3$He and $^4$He densities under these operating conditions are 0.09 g/cm$^3$ and 0.15 g/cm$^3$, respectively. The resulting luminosities for a canonical beam current of 100 $\mu$A are $2.2 \times 10^{38}$ cm$^{-2}$s$^{-1}$ for $^3$He and $2.8 \times 10^{38}$ cm$^{-2}$s$^{-1}$ for $^4$He. To eliminate background electrons from

quasielastic scattering off the Al end-caps of the $^4$He target cell, two tungsten collimating slits will be mounted on the support frame of the target cell toward the spectrometer side. The slits will mask the spectrometer from the end-caps and at the same time will define the effective target length seen by the spectrometer.

The single- and double-arm effective solid angle for the evaluation of the cross sections has been determined by means of a Monte Carlo simulation method of elastic electron-nucleus scattering [39] with the two HRS spectrometers, as in the coincidence elastic electron-deuteron E91-26 JLab experiment. The solid angle values assumed in the proposal were evaluated by this method. The double-arm solid angle for the $^3$He backward (forward) measurements has been estimated to be $\sim$ 10 (2) msr, on the average. The single-arm solid angle for the $^4$He measurements has been estimated to be $\sim$ 6 msr, on the average. The simulation has also shown that the elastic electron-$^4$He peak of the single-arm measurements will be clearly separated from the inelastic background, as can be seen in Figure 8. Plotted in the figure is, for the highest $Q^2$ kinematics (worst case), the excitation energy, $\omega = W - M$, spectrum of scattered electrons, where $W$ is the invariant mass of the final hadronic state, $W = [M^2 + 2M(E - E') - Q^2]^{1/2}$. The simulation took into account the effects of Landau ionization energy loss, internal and external bremsstrahlung radiation and multiple scattering for both incident and scattered electrons. The excitation energy resolution will be dominated by Landau straggling in the target. Contributions from the beam energy spread and the spectrometer angular and momentum resolutions will be negligible.

The calibration of the single- and double-arm experimental set-up will be checked and monitored with single-arm and double-arm electron-proton (e-p) elastic scattering. The e-p kinematics for the double-arm scattering will be such as to match the electron-He solid angle Jacobian. This will constitute a powerful means of controlling the normalization of the double-arm electron-He scattering. Any possible contribution to the $^3$He double-arm cross sections coming from the Al target end-caps will be measured in special runs with an empty replica target. It is expected, as in the case of the elastic electron-deuteron E91-26 experiment, that the hydrogen and aluminum runs will require 20% of the total running time.

To calculate counting rates, projected statistical uncertainties and required beam times, we used the above stated luminosity and solid angle assumptions, and an approximate radiative correction factor of 0.7. Figures 9 and 10 show the quality of the projected data for the $^3$He charge and magnetic form factor measurements, assuming that they are described, at large $Q^2$, by the model of Schiavilla and collaborators [8, 9]. The sensitivity limit for the $^3$He charge and magnetic form factors is estimated to be $\sim 2 \times 10^{-5}$ and $\sim 1 \times 10^{-5}$, respectively. The sensitivity limit is defined as the lowest form factor value that can be measured with $\sim \pm 30\%$ statistical error in about a week of beam time for both forward and backward measurements. The estimated cross sections, counting rates, running times and projected statistical uncertainties in the extraction of the two $^3$He form factors are given, for this model, in Table 4.

Fig. 11 shows the sensitivity limit for the $^3$He $F \equiv \sqrt{A(Q^2)}$ form factor. The sensitivity limit is again defined as a $\sim \pm$ 30% measurement in a week of beam time at a given $Q^2$ kinematics. The experiment will be able to provide precise $F$ data for $^3$He over the $Q^2$ range of the previous SLAC measurements and beyond. The latter measurements [33] were performed at a single forward scattering angle ($\Theta = 8^\circ$) and were not able to separate the two form factors. Shown also in the figure are the complete (IA+MEC) calculation of Schiavilla and collaborators [8, 9], and the prediction of the dimensional-scaling quark model of Brodsky and Chertok [24], arbitrarily normalized at $\sim 50$ fm$^{-2}$. The existing $F$ data for $^3$He strongly suggest a change of slope at about $Q^2 = 55$ fm$^{-2}$, that can be attributed to a possible diffraction minimum, or to the onset of quark dimensional-scaling as argued by Chertok [40].

Figure 12 shows the quality of the projected data for the $^4$He charge form factor, assuming a linear extrapolation of the existing data, along with theoretical predictions at large momentum transfers. The variational Monte Carlo calculations by Wiringa [10] and Schiavilla and collaborators [9], shown in the figure, predict a second diffraction minimum that would be measurable by this experiment. Also shown in the figure is the asymptotic prediction of the dimensional-scaling quark model by Brodsky and Chertok [24], arbitrarily normalized at $\sim 40$ fm$^{-2}$. The estimated cross sections, counting rates, running times and projected statistical uncertainties in the extraction of the $^4$He form factor are given in Table 5.

It is evident, from Figures 9, 10, 11 and 12, that this experiment will significantly advance our knowledge of the form factors of the three- and four-body systems. The expected data will extend our $^3$He and $^4$He form factor knowledge down by one to two orders in magnitude and out in $Q^2$ by possibly more than a factor of two. The run plan scenarios of Tables 4 and 5 dictate that the required beam time for each form factor measurement be 15 days (including 3 days of proton calibrations and empty target runs). The proposed measurements will be able to uncover the predicted second diffraction minima of the $^3$He and $^4$He form factors or explore a possible asymptotic fall-off indicative of a transition from meson-nucleon to quark-gluon degrees of freedom.

## 3 Summary

In summary, this is a proposal to measure the charge and magnetic form factors of $^3$He and $^4$He up to the largest momentum transfer possible in the JLab Hall A Facility. We request 45 days of beam time with beam energies between 0.5 and 4.5 GeV and current of 100 $\mu$A. The expected data will extend our form-factor knowledge down by one to two orders in magnitude and out in $Q^2$ by possible more than a factor of two. The experiment will produce data of fundamental importance to the understanding and advancement of modern few-body nuclear physics.

## References


[1] L. E. Marcucci, D. O. Riska and R. Schiavilla, Phys. Rev. **C58**, 3069 (1998).

[2] For a review see: J. Carlson and R. Schiavilla, Rev. Mod. Phys. **70**, 743 (1998).

[3] For a review see: C. E. Carlson, J. R. Hiller, R. J. Holt, Annu. Rev. Nucl. Part. Sci. **47**, 395 (1997).

[4] R. A. Brandenburg, Y. E. Kim and A. Tubis, Phys. Rec. **C12**, 1368 (1975).

[5] W. Strueve, Ch. Hajduk, P. U. Sauer and W. Theis, Nucl. Phys. **A465**, 651 (1987).

[6] A. Laverne and C. Gignoux, Nucl. Phys. **A203**, 597 (1973).

[7] E. Hadjimichael, B. Goulard and R. Bornais, Phys. Rev. **C27**, 831 (1983); E. Hadjimichael, Phys. Lett. **B172**, 156 (1986).

[8] R. Schiavilla, V. R. Pandharipande and D. O. Riska, Phys. Rev. **C40**, 2294 (1989); R. Schiavilla and D. O. Riska, Phys. Lett. **B244**, 373 (1990).

[9] R. Schiavilla, V. R. Pandharipande and D. O. Riska, Phys. Rev. **C41**, 309 (1990).

[10] R. B. Wiringa, Phys. Rev. **C43**, 1585 (1991).

[11] M. J. Musolf, R. Schiavilla and T. W. Donnely, Phys. Rev. **C50**, 2173 (1994).

[12] J. Carlson, Phys. Rev. **C38**, 1879 (1988).

[13] D. O. Riska, Phys. Rep. **181**, 207 (1989).

[14] A. Picklesimer, R. A. Rice and R. Brandenburg, Phys. Rev. Lett. **68**, 1484 (1992).

[15] J. Lomnitz-Adler, V. R. Pandharipande and R. A. Smith, Nucl. Phys. **A361**, 399 (1981).

[16] J. L. Friar *et al.*, Ann. Rev. Nucl. Part. Sci. **34**, 403 (1984); preprint nuc-th-0005076, to appear in Nucl. Phys. **A** (2000).

[17] J. L. Friar, B. F. Gibson and G. L. Payne, Phys. Rev. **C35**, 1502 (1987).

[18] T. Katayama, Y. Akaishi and H. Tanaka, Prog. Theor. Phys. **67**, 236 (1982).

[19] M. Namiki, K. Okano and N. Oshimo, Phys. Rev. **C25**, 2157 (1982).

[20] V. V. Burov and V. K. Lukyanov and A. I. Titov, Z. Phys. **A318**, 67 (1984); V. V. Burov and V. K. Lukyanov, Nucl. Phys. **A463**, 263c (1987).

[21] M. A. Maize and Y. E. Kim, Phys. Rev. **C31**, 1923 (1985).

[22] L. S. Kisslinger, W.-H. Ma and P. Hoodbhoy, Nucl. Phys. **A459**, 645 (1986); W.-H. Ma and L. S. Kisslinger, Nucl. Phys. **A531**, 493 (1991).

[23] H. Dijk and M. Beyer, Phys. Lett. **B237**, 323 (1990).

[24] S. J. Brodsky and B. T. Chertok, Phys. Rev. Lett. **37**, 269 (1976); Phys. Rev. **D14**, 3003 (1976).

[25] H. Collard *et al.*, Phys. Rev. **138**, B57 (1965).

[26] J. S. McCarthy, I. Sick and R. R. Whitney, Phys. Rev. **C15**, 1396 (1977).

[27] M. Bernheim *et al.*, Lett. Nuovo Cimento **5**, 431 (1972).

[28] J. M. Cavedon *et al.*, Phys. Rev. Lett. **49**, 987 (1982).

[29] A. Amroun *et al.*, Phys. Rev. Lett. **69**, 253 (1992); Nucl. Phys. **A579**, 596 (1994).

[30] P. C. Dunn *et al.*, Phys. Rev. **C27**, 71 (1983).

[31] D. H. Beck *et al.*, Phys. Rev. **C30**, 1403 (1984).

[32] C. R. Ottermann *et al.*, Nucl. Phys. **A436**, 688 (1985).

[33] R. G. Arnold *et al.*, Phys. Rev. Lett. **40**, 1429 (1978).

[34] H. Henning, P. U. Sauer and W. Theis, Nucl. Phys. **A537**, 367 (1992).

[35] G. Rupp and J. A. Tjon, Phys. Rev. **C45**, 2133 (1992).

[36] A. Stadler, F. Gross and M. Frank, Phys. Rev. **C56**, 2396 (1997).

[37] R. F. Frosch *et al.*, Phys. Rev. **160**, 874 (1967).

[38] L. C. Alexa *et al.*, Phys. Rev. Lett. **82**, 1374 (1999).

[39] A. T. Katramatou, SLAC Report SLAC-NPAS-TN-86-08 (1986).

[40] B. T. Chertok, Phys. Rev. Lett. **41**, 1155 (1978).

## $^3$He Forward Kinematics

| $Q^2$ ($\mathrm{fm}^{-2}$) | $E$ (GeV) | $E'$ (GeV) | $\Theta$ (deg.) | $P_r$ (GeV/c) | $\Theta_r$ (deg.) | $(\Delta\Omega)_e/(\Delta\Omega)_r$ |
|---|---|---|---|---|---|---|
| 19.8 | 3.6 | 3.463 | 14.3 | 0.888 | 74.1 | 0.24 |
| 25.2 | 3.6 | 3.425 | 16.2 | 1.006 | 72.0 | 0.28 |
| 31.3 | 3.6 | 3.383 | 18.2 | 1.125 | 69.9 | 0.32 |
| 34.5 | 3.6 | 3.361 | 19.2 | 1.184 | 68.9 | 0.35 |
| 37.9 | 3.6 | 3.337 | 20.2 | 1.243 | 67.9 | 0.37 |
| 41.5 | 3.6 | 3.313 | 21.2 | 1.303 | 66.9 | 0.39 |
| 45.1 | 3.6 | 3.287 | 22.2 | 1.362 | 65.9 | 0.42 |
| 48.9 | 3.6 | 3.261 | 23.2 | 1.421 | 64.9 | 0.45 |
| 52.8 | 4.4 | 4.034 | 19.6 | 1.480 | 66.1 | 0.33 |
| 55.0 | 4.4 | 4.019 | 20.0 | 1.512 | 65.6 | 0.34 |
| 56.9 | 4.4 | 4.006 | 20.4 | 1.540 | 65.2 | 0.35 |
| 61.0 | 4.4 | 3.977 | 21.2 | 1.599 | 64.3 | 0.37 |
| 65.3 | 4.4 | 3.947 | 22.1 | 1.658 | 63.4 | 0.39 |
| 69.7 | 4.4 | 3.917 | 22.9 | 1.717 | 62.5 | 0.42 |
| 74.2 | 4.4 | 3.885 | 23.7 | 1.776 | 61.7 | 0.44 |
| 78.9 | 4.4 | 3.853 | 24.6 | 1.836 | 60.8 | 0.47 |
| 83.6 | 4.4 | 3.821 | 25.4 | 1.895 | 59.9 | 0.49 |
| 88.4 | 4.4 | 3.787 | 26.3 | 1.954 | 59.1 | 0.52 |

Table 1: Incident beam, scattered electron and recoil nucleus kinematics for the forward $^3$He measurements.

**$^3$He Backward Kinematics**

| $Q^2$ (fm$^{-2}$) | $E$ (GeV) | $E'$ (GeV) | $\Theta$ (deg.) | $P_r$ (GeV/c) | $\Theta_r$ (deg.) | $(\Delta\Omega)_e/(\Delta\Omega)_r$ |
|---|---|---|---|---|---|---|
| 19.8 | 0.535 | 0.398 | 144.0 | 0.888 | 15.3 | 5.17 |
| 25.2 | 0.616 | 0.441 | 144.0 | 1.006 | 14.9 | 5.39 |
| 31.3 | 0.699 | 0.482 | 144.0 | 1.125 | 14.6 | 5.63 |
| 34.5 | 0.741 | 0.502 | 144.0 | 1.184 | 14.4 | 5.75 |
| 37.9 | 0.784 | 0.521 | 144.0 | 1.243 | 14.3 | 5.88 |
| 41.5 | 0.827 | 0.540 | 144.0 | 1.303 | 14.1 | 6.01 |
| 45.1 | 0.871 | 0.558 | 144.0 | 1.362 | 13.9 | 6.14 |
| 48.9 | 0.915 | 0.576 | 144.0 | 1.421 | 13.8 | 6.28 |
| 52.8 | 0.959 | 0.593 | 144.0 | 1.480 | 13.6 | 6.42 |
| 55.0 | 0.983 | 0.602 | 144.0 | 1.512 | 13.5 | 6.49 |
| 56.9 | 1.004 | 0.610 | 144.0 | 1.540 | 13.5 | 6.56 |
| 61.0 | 1.049 | 0.626 | 144.0 | 1.599 | 13.3 | 6.70 |
| 65.3 | 1.095 | 0.642 | 144.0 | 1.658 | 13.2 | 6.85 |
| 69.7 | 1.141 | 0.658 | 144.0 | 1.717 | 13.0 | 7.00 |
| 74.2 | 1.188 | 0.673 | 144.0 | 1.776 | 12.9 | 7.15 |
| 78.9 | 1.234 | 0.688 | 144.0 | 1.836 | 12.7 | 7.31 |
| 83.6 | 1.282 | 0.702 | 144.0 | 1.895 | 12.6 | 7.47 |
| 88.4 | 1.329 | 0.716 | 144.0 | 1.954 | 12.4 | 7.63 |

Table 2: Incident beam, scattered electron and recoil nucleus kinematics for the backward $^3$He measurements.

**$^4$He Kinematics**

| $Q^2$ ($fm^{-2}$) | $E$ (GeV) | $E'$ (GeV) | $\Theta$ (deg.) | $P_r$ (GeV/c) | $\Theta_r$ (deg.) | $(\Delta\Omega)_e/(\Delta\Omega)_r$ |
|---|---|---|---|---|---|---|
| 9.0 | 1.508 | 1.461 | 23.0 | 0.594 | 74.1 | 0.60 |
| 14.0 | 1.889 | 1.816 | 23.0 | 0.742 | 73.0 | 0.57 |
| 19.0 | 2.207 | 2.108 | 23.0 | 0.866 | 72.1 | 0.55 |
| 24.0 | 2.488 | 2.363 | 23.0 | 0.975 | 71.3 | 0.53 |
| 29.0 | 2.742 | 2.590 | 23.0 | 1.073 | 70.6 | 0.52 |
| 34.0 | 2.976 | 2.798 | 23.0 | 1.164 | 69.9 | 0.50 |
| 39.0 | 3.194 | 2.990 | 23.0 | 1.249 | 69.3 | 0.49 |
| 44.0 | 3.400 | 3.170 | 23.0 | 1.329 | 68.7 | 0.49 |
| 49.0 | 3.595 | 3.339 | 23.0 | 1.405 | 68.2 | 0.48 |
| 54.0 | 3.781 | 3.498 | 23.0 | 1.477 | 67.7 | 0.47 |
| 59.0 | 3.959 | 3.650 | 23.0 | 1.547 | 67.2 | 0.46 |
| 64.0 | 4.130 | 3.796 | 23.0 | 1.614 | 66.8 | 0.46 |
| 69.0 | 4.295 | 3.935 | 23.0 | 1.678 | 66.4 | 0.45 |
| 74.0 | 4.455 | 4.068 | 23.0 | 1.741 | 65.9 | 0.45 |

Table 3: Incident beam, scattered electron and recoil nucleus kinematics for the $^4$He measurements.

## $^3$He Run Plan

| $Q^2$ (fm$^{-2}$) | $[d\sigma/d\Omega)]_f$ (nb/sr) | $N_f$ | $T_f$ (h) | $[d\sigma/d\Omega)]_b$ (nb/sr) | $N_b$ | $T_b$ (h) | $F_C$ | $\Delta F_C$ ($\pm$%) | $F_M$ | $\Delta F_M$ ($\pm$%) |
|---|---|---|---|---|---|---|---|---|---|---|
| 19.8 | 1.4E-1 | 32768 | 0.3 | 2.2E-4 | 2048 | 1.7 | 4.7E-3 | 0.3 | 1.6E-3 | 3.2 |
| 25.2 | 4.3E-2 | 16384 | 0.4 | 9.7E-5 | 1024 | 1.9 | 3.4E-3 | 0.4 | 1.3E-3 | 3.4 |
| 31.3 | 8.9E-3 | 8192 | 1.1 | 2.9E-5 | 1024 | 6.3 | 1.9E-3 | 0.6 | 7.9E-4 | 2.9 |
| 34.5 | 3.7E-3 | 4096 | 1.3 | 1.3E-5 | 512 | 6.9 | 1.4E-3 | 0.9 | 5.5E-4 | 4.0 |
| 37.9 | 1.4E-3 | 2048 | 1.7 | 5.3E-6 | 256 | 8.6 | 9.5E-4 | 1.2 | 3.5E-4 | 5.8 |
| 41.5 | 4.8E-4 | 512 | 1.3 | 1.9E-6 | 128 | 12.0 | 6.2E-4 | 2.4 | 2.1E-4 | 8.7 |
| 45.1 | 1.5E-4 | 512 | 4.1 | 6.2E-7 | 64 | 18.3 | 3.8E-4 | 2.5 | 1.2E-4 | 12.0 |
| 48.9 | 3.6E-5 | 256 | 8.3 | 1.5E-7 | 32 | 38.3 | 2.1E-4 | 3.4 | 5.8E-5 | 19.2 |
| 52.8 | 9.3E-6 | 64 | 8.1 | 1.4E-8 | 2 | 25.5 | 9.3E-5 | 6.6 | 5.2E-6 | DF |
| 55.0 | 1.8E-6 | 16 | 10.3 | 1.1E-8 | 2 | 33.3 | 4.0E-5 | 16.9 | 2.0E-5 | 47.8 |
| 56.9 | 2.4E-6 | 4 | 1.9 | 6.9E-8 | 8 | 20.5 | 1.4E-5 | DF | 5.8E-5 | 18.7 |
| 61.0 | 6.1E-6 | 8 | 1.5 | 1.6E-7 | 8 | 8.8 | 4.0E-5 | DF | 9.0E-5 | 18.9 |
| 65.3 | 8.0E-6 | 256 | 37.8 | 2.0E-7 | 32 | 28.7 | 6.0E-5 | 24.3 | 1.0E-4 | 9.5 |
| 69.7 | 7.9E-6 | 256 | 38.3 | 1.9E-7 | 32 | 29.8 | 7.1E-5 | 18.8 | 1.0E-4 | 9.6 |
| 74.2 | 6.6E-6 | 256 | 45.7 | 1.7E-7 | 32 | 33.2 | 6.9E-5 | 19.6 | 9.7E-5 | 9.6 |
| 78.9 | 5.4E-6 | 256 | 55.9 | 1.5E-7 | 32 | 37.8 | 6.6E-5 | 20.7 | 9.2E-5 | 9.5 |
| 83.6 | 3.8E-6 | 128 | 39.9 | 1.1E-7 | 32 | 50.1 | 5.8E-5 | 24.3 | 8.2E-5 | 9.5 |
| 88.4 | 2.0E-6 | 64 | 38.4 | 6.3E-8 | 16 | 45.1 | 4.4E-5 | 36.3 | 6.2E-5 | 13.5 |

Table 4: A run plan scenario for the $^3$He forward ($f$) and backward ($b$) measurements, assuming that the charge and magnetic form factors follow the model of Schiavilla and collaborators [8, 9]. Here, $N$ and $T$ denote the expected number of elastic events and the required beam time, and DF a diffraction minimum. The form factor errors represent statistical uncertainties.

**$^4$He Run Plan**

| $Q^2$ ($\mathrm{fm}^{-2}$) | $d\sigma/d\Omega$ (nb/sr) | $T$ (h) | $N$ | $F_C$ | $\Delta F_C$ ($\pm$%) |
|---|---|---|---|---|---|
| 9.0 | 1.3E-1 | 0.1 | 14183 | 5.0E-3 | 0.4 |
| 14.0 | 2.8E-1 | 0.1 | 20310 | 9.0E-3 | 0.4 |
| 19.0 | 9.6E-2 | 0.1 | 12006 | 6.2E-3 | 0.5 |
| 24.0 | 1.8E-2 | 0.1 | 5212 | 3.1E-3 | 0.7 |
| 29.0 | 3.6E-3 | 0.2 | 2315 | 1.5E-3 | 1.0 |
| 34.0 | 7.3E-4 | 0.3 | 1044 | 7.4E-4 | 1.5 |
| 39.0 | 1.5E-4 | 0.7 | 476 | 3.6E-4 | 2.3 |
| 44.0 | 3.2E-5 | 1.6 | 219 | 1.8E-4 | 3.3 |
| 49.0 | 6.9E-6 | 3.5 | 101 | 8.7E-5 | 4.9 |
| 54.0 | 1.5E-6 | 7.4 | 47 | 4.3E-5 | 7.0 |
| 59.0 | 3.3E-7 | 15.8 | 22 | 2.1E-5 | 10.1 |
| 64.0 | 7.2E-8 | 39.2 | 12 | 1.0E-5 | 13.5 |
| 69.0 | 1.6E-8 | 88.3 | 6 | 5.1E-6 | 18.7 |
| 74.0 | 3.6E-9 | 131.9 | 2 | 2.5E-6 | 30.7 |

Table 5: A run plan scenario for the $^4$He measurements, assuming that the charge form factor is desribed by a linear extrapolation of the existing SLAC data [33]. Here, $N$ and $T$ denote the expected number of single-arm elastic events and the required beam time. The form factor error is statistical.

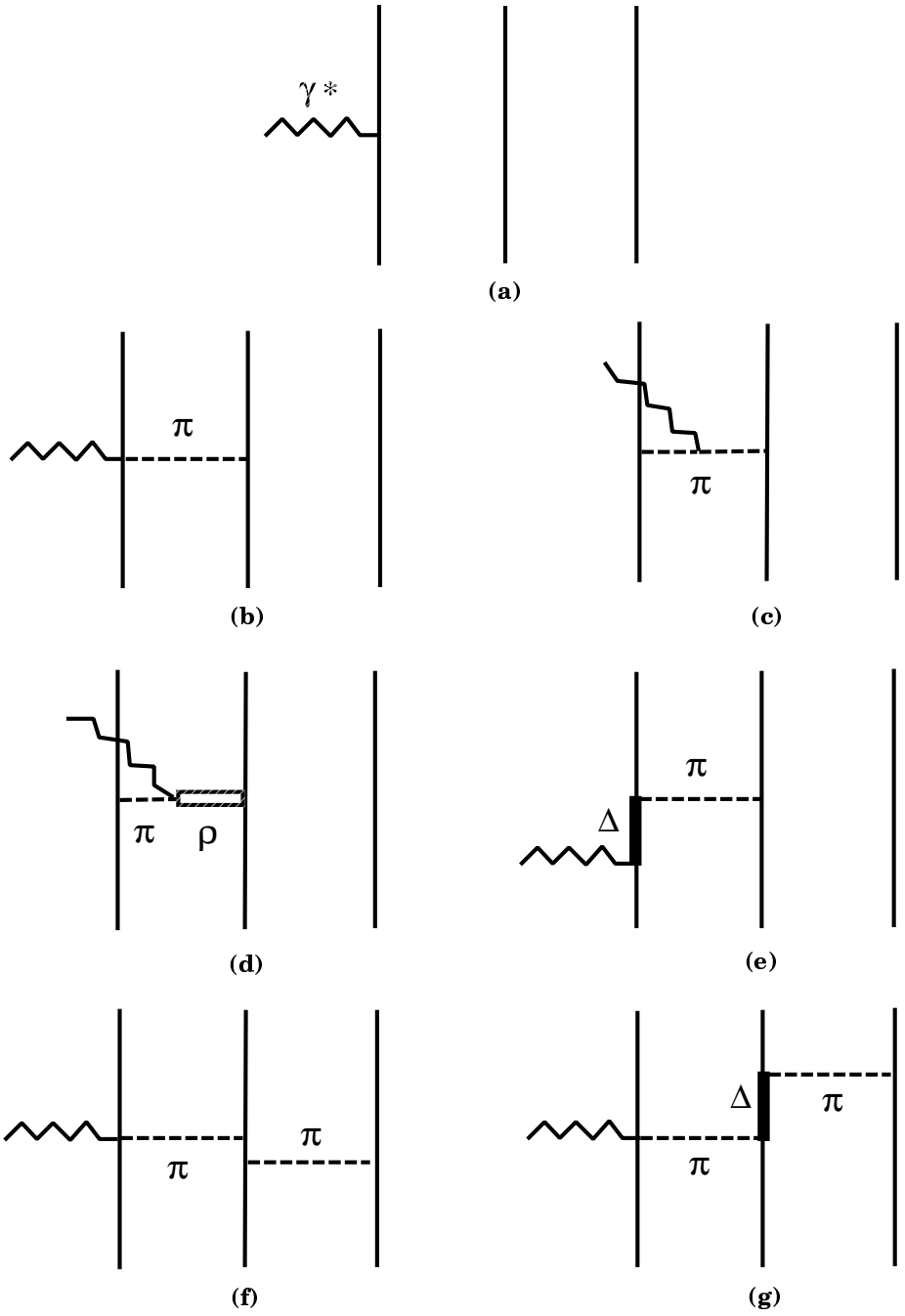


Figure 1: Selected diagrams contributing to elastic electron-$^3$He scattering: impulse approximation (a); "model-independent" meson-exchange currents (b,c); "model-dependent" meson-exchange currents (d,e); three-body force contributions (f,g) [2].

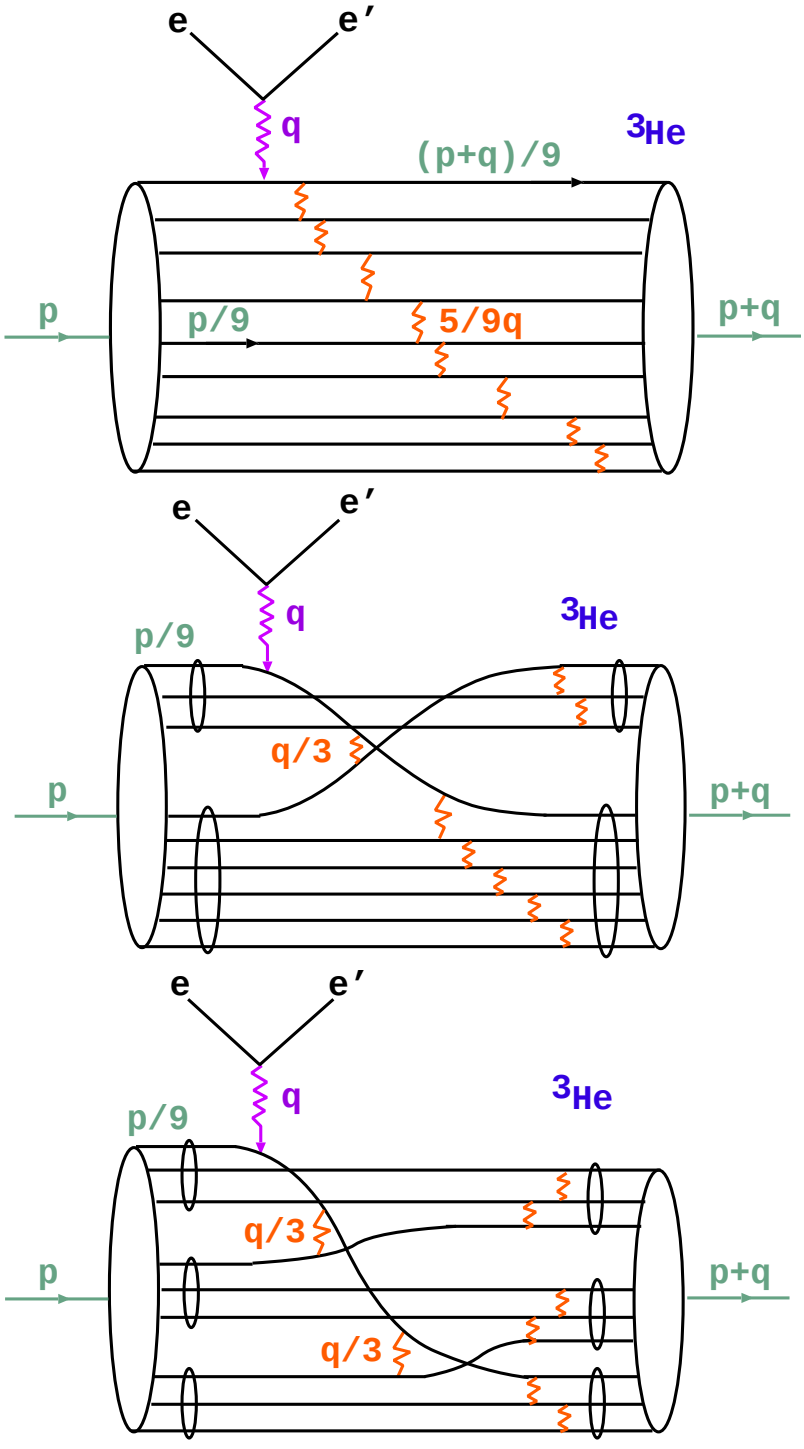


Figure 2: Elastic electron-$^3$He scattering in the dimensional-scaling quark model of Brodsky and Chertok [24]: a) democratic nine-quark chain; b) nucleon-dinucleon quark interchange; c) three-nucleon quark interchange.

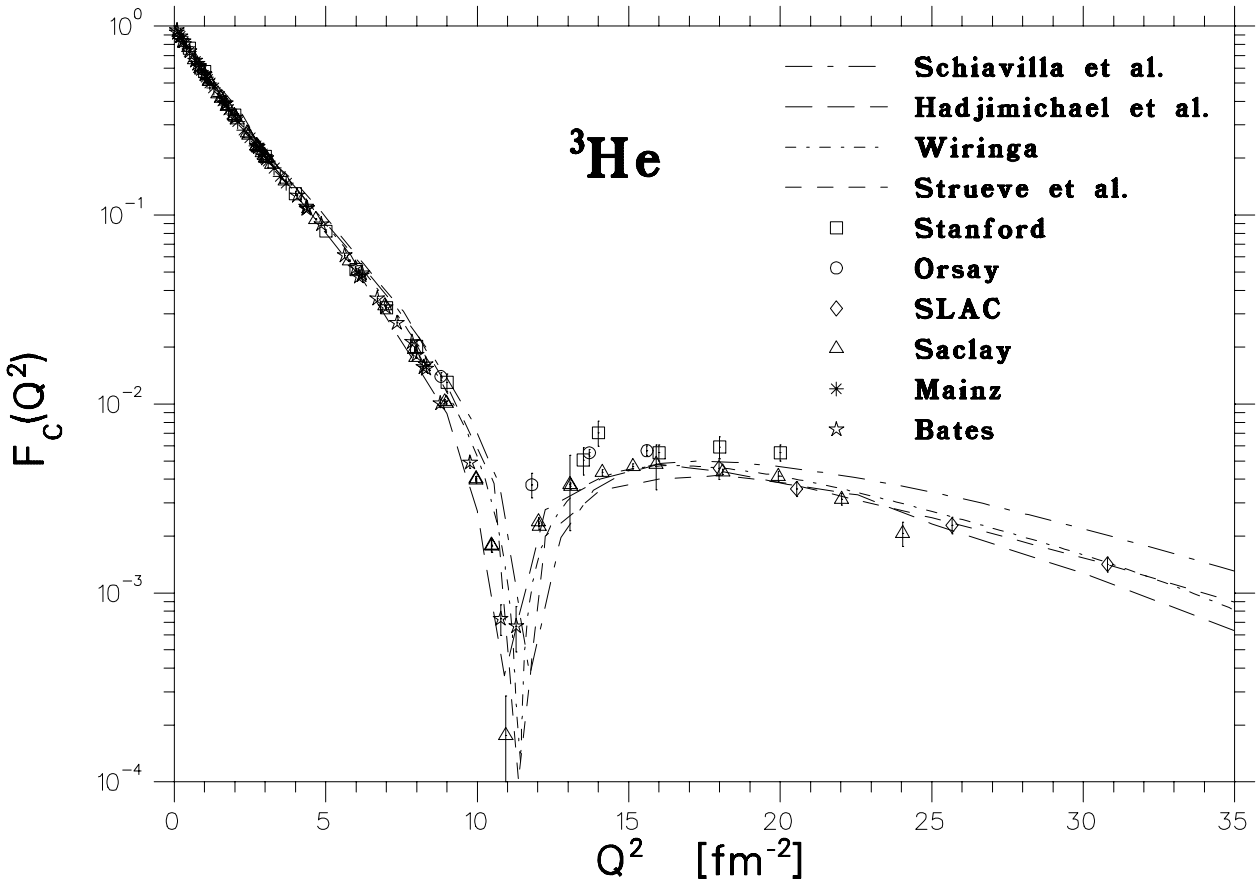


Figure 3: $^3$He charge form factor data from Stanford [25, 26], Orsay [27], SLAC [33], Saclay [29], Mainz [32] and Bates [31] experiments, and theoretical IA+MEC calculations by Schiavilla *et al.* [9], Hadjimichael *et al.* [7], Strueve *et al.* [5] and Wiringa [10].

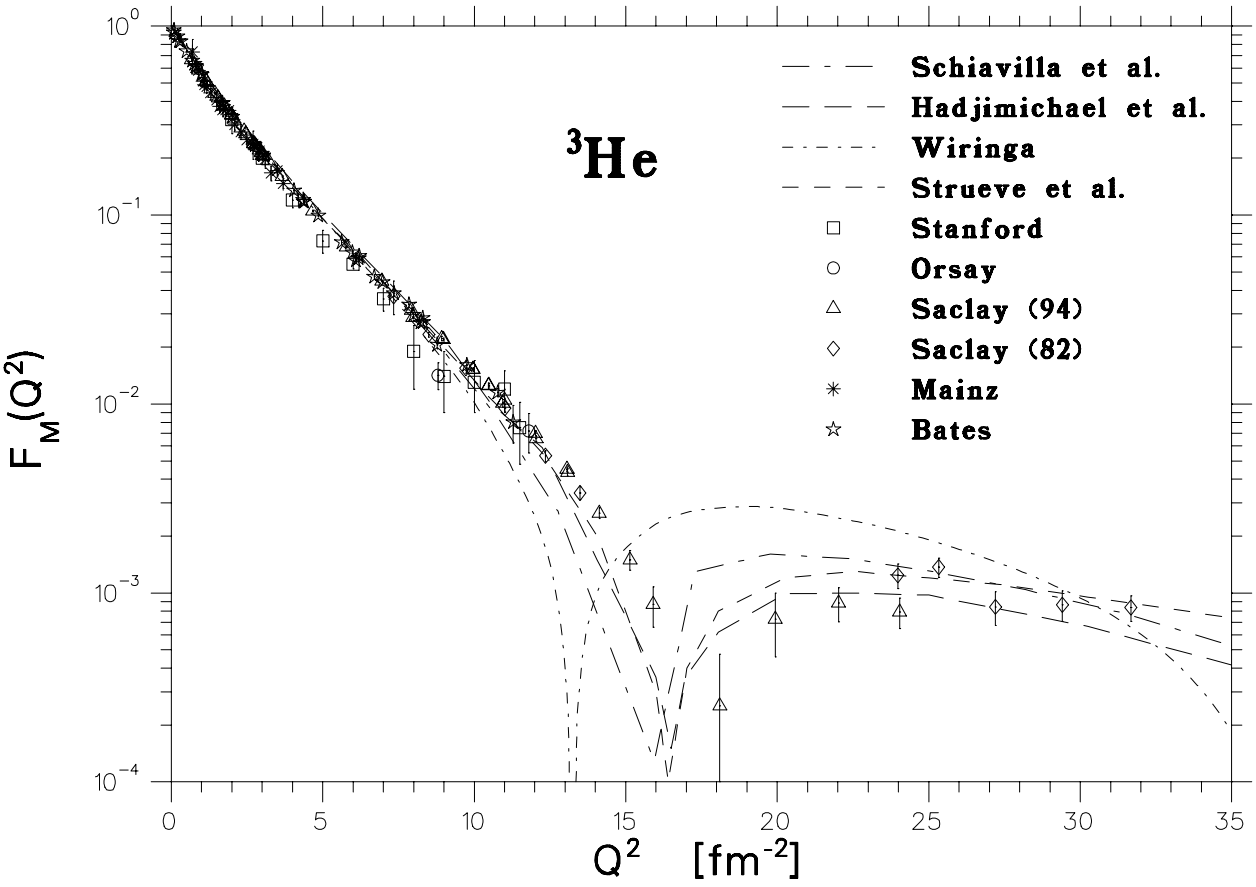


Figure 4: $^3$He magnetic form factor data from Stanford [25, 26], Saclay [28],[29], Mainz [32], Orsay [27] and Bates [30] experiments, and theoretical IA+MEC calculations by Schiavilla *et al.* [8], Hadjimichael *et al.* [7], Strueve *et al.* [5] and Wiringa [10].

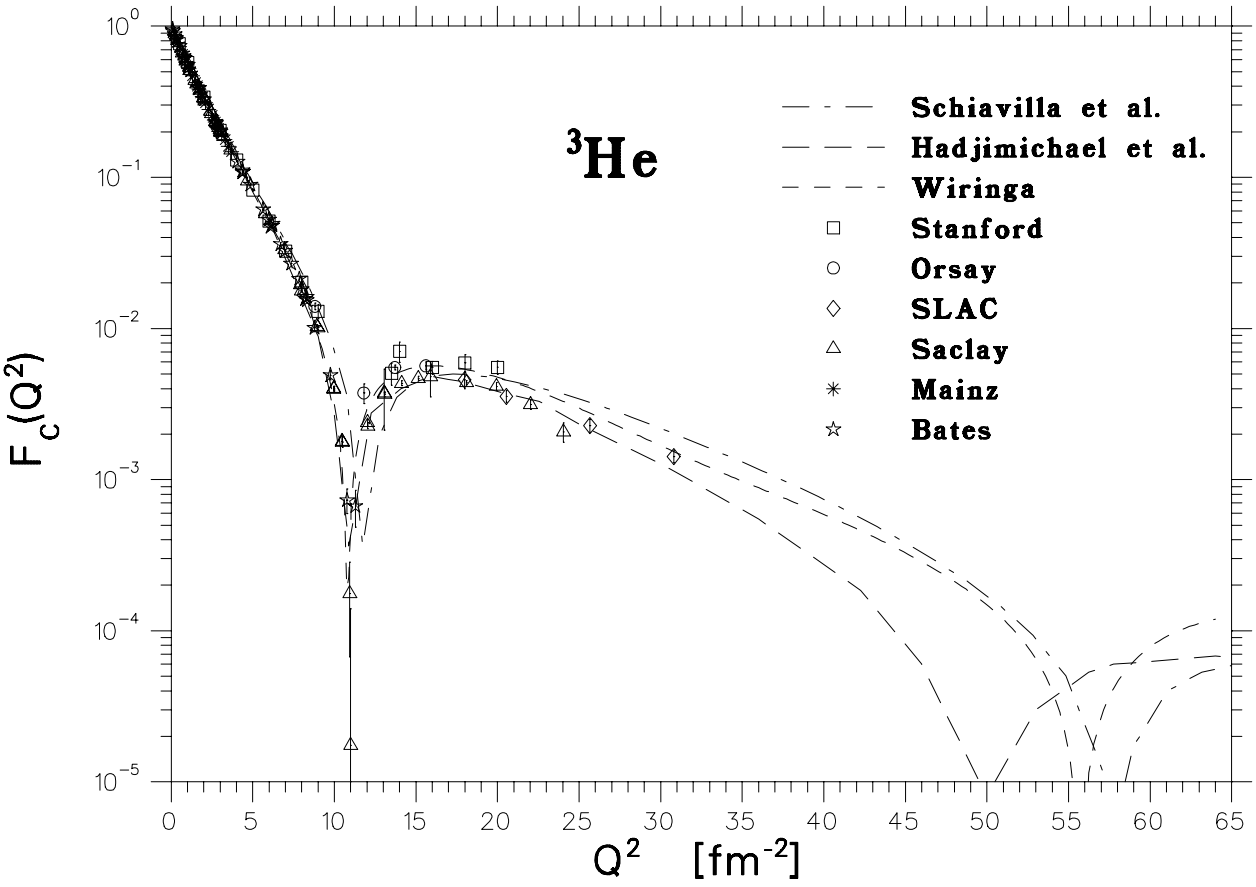


Figure 5: $^3$He charge form factor data from Stanford [25, 26], Orsay [27], SLAC [33], Mainz [32], Saclay [29] and Bates [31] experiments, and theoretical IA+MEC calculations, for large $Q^2$, by Schiavilla *et al.* [9], Hadjimichael *et al.* [7] and Wiringa [10].

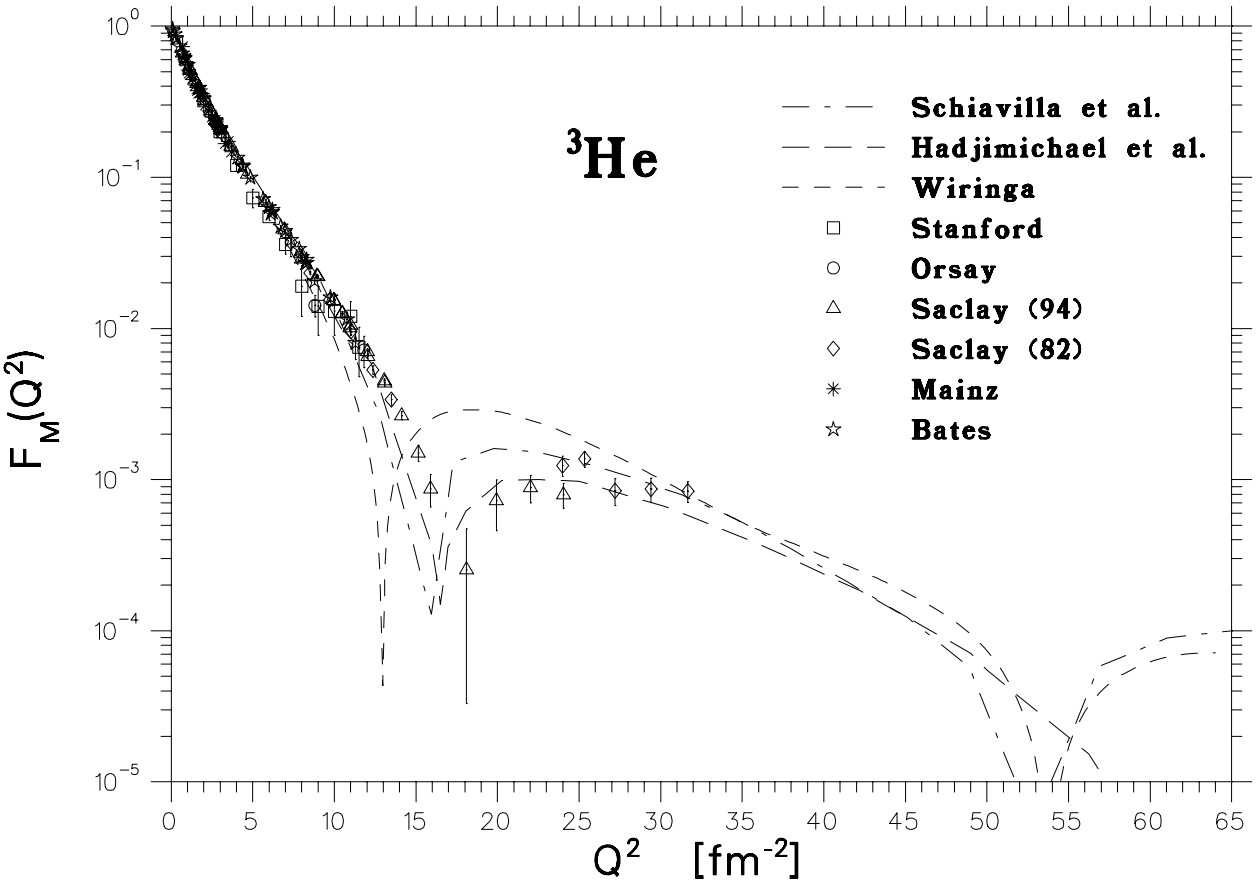


Figure 6: $^3$He magnetic form factor data from Stanford [25, 26], Saclay [28],[29], Mainz [32], Orsay [27] and Bates [30] experiments, and theoretical IA+MEC calculations, for large $Q^2$, by Schiavilla *et al.* [8], Hadjimichael *et al.* [7] and Wiringa [10].

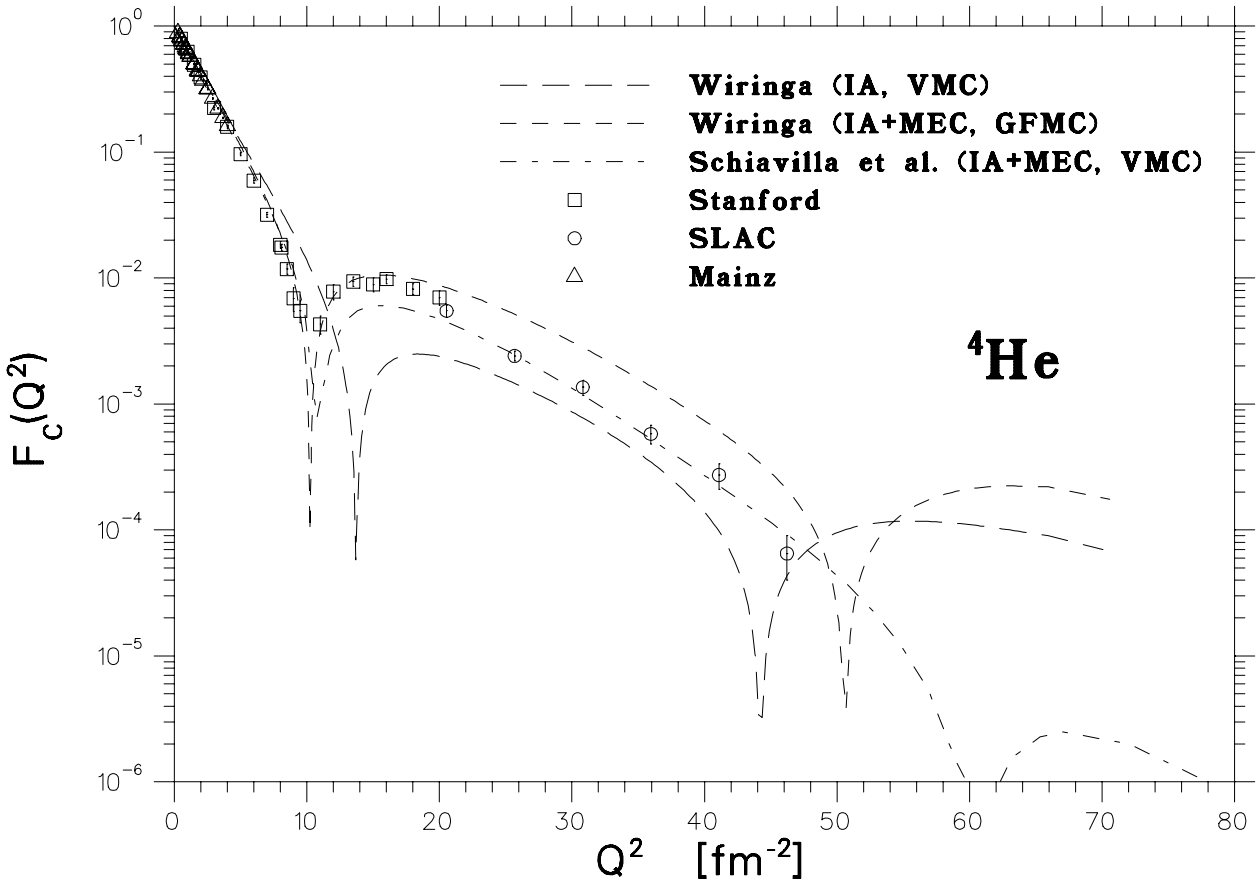


Figure 7: $^4$He charge form factor data from Stanford [37, 26], Mainz [32] and SLAC [33], and variational Monte Carlo (VMC) and Green's Function Monte Carlo (GFMC) calculations by Schiavilla *et al.* [9] and Wiringa [10].

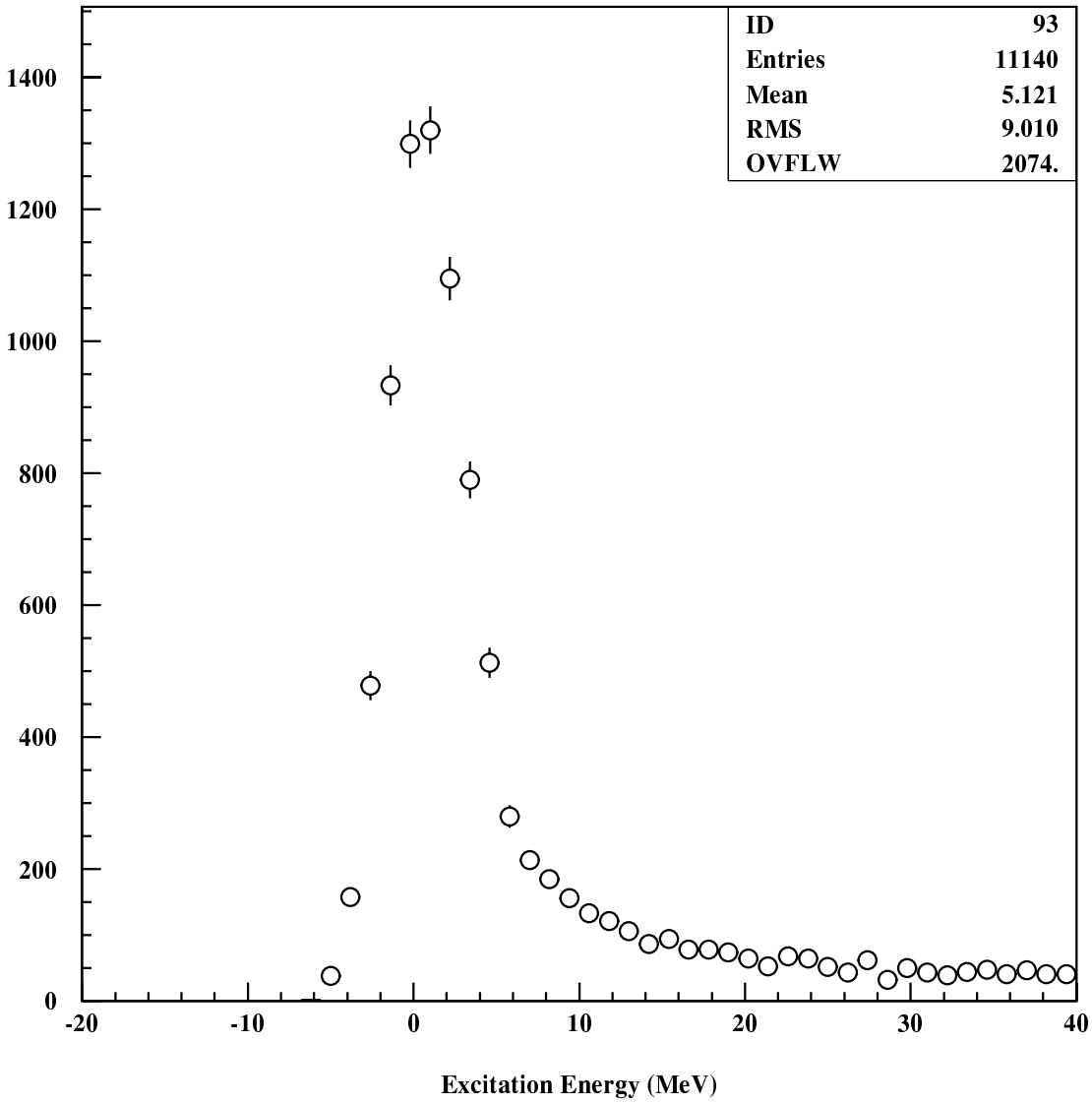


Figure 8: The excitation energy peak from our Monte Carlo simulation for the highest single-arm elastic electron-$^4$He $Q^2$ setting ($Q^2 = 74$ fm$^{-2}$). The inelastic break-up threshold is at 20 MeV.

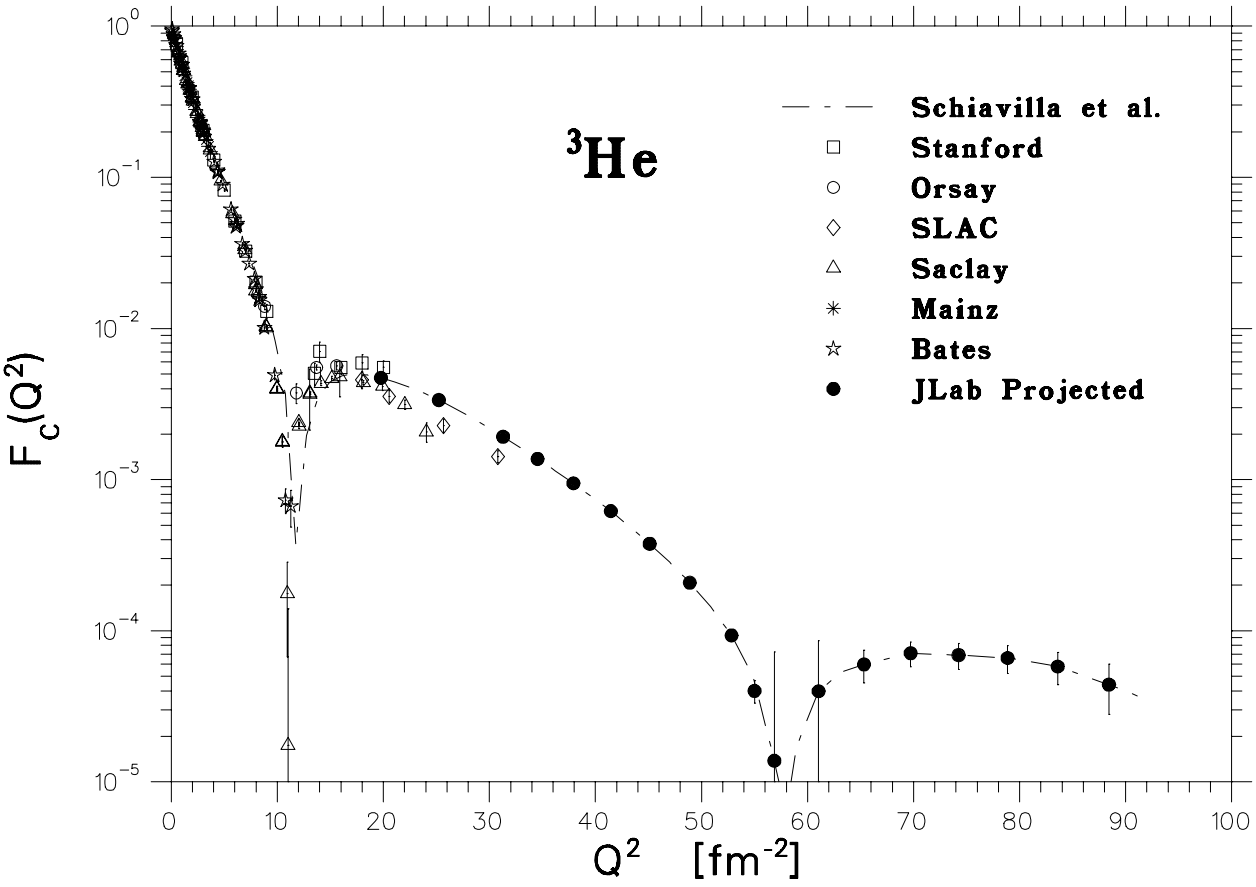


Figure 9: $^3$He charge form factor projected data from this experiment. Also shown are data from Stanford [25, 26], Orsay [27], SLAC [33], Saclay [29], Mainz [32] and Bates [31] experiments, and the theoretical IA+MEC calculation by Schiavilla *et al.* [9].

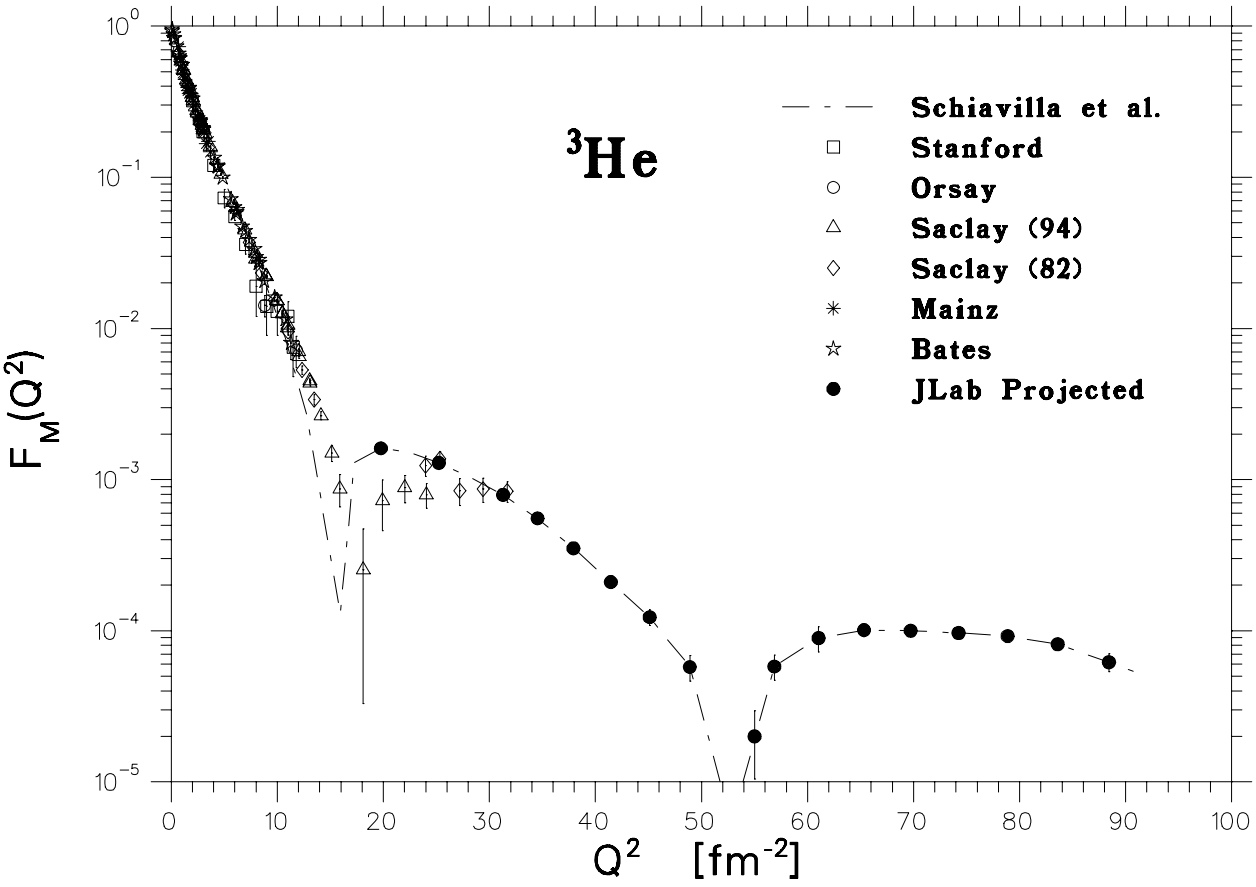


Figure 10: $^3$He magnetic form factor projected data from this experiment. Also shown are data from Stanford [25, 26], Saclay [28, 29], Mainz [32], Orsay [27] and Bates [30] experiments, and the theoretical IA+MEC calculation by Schiavilla *et al.* [8].

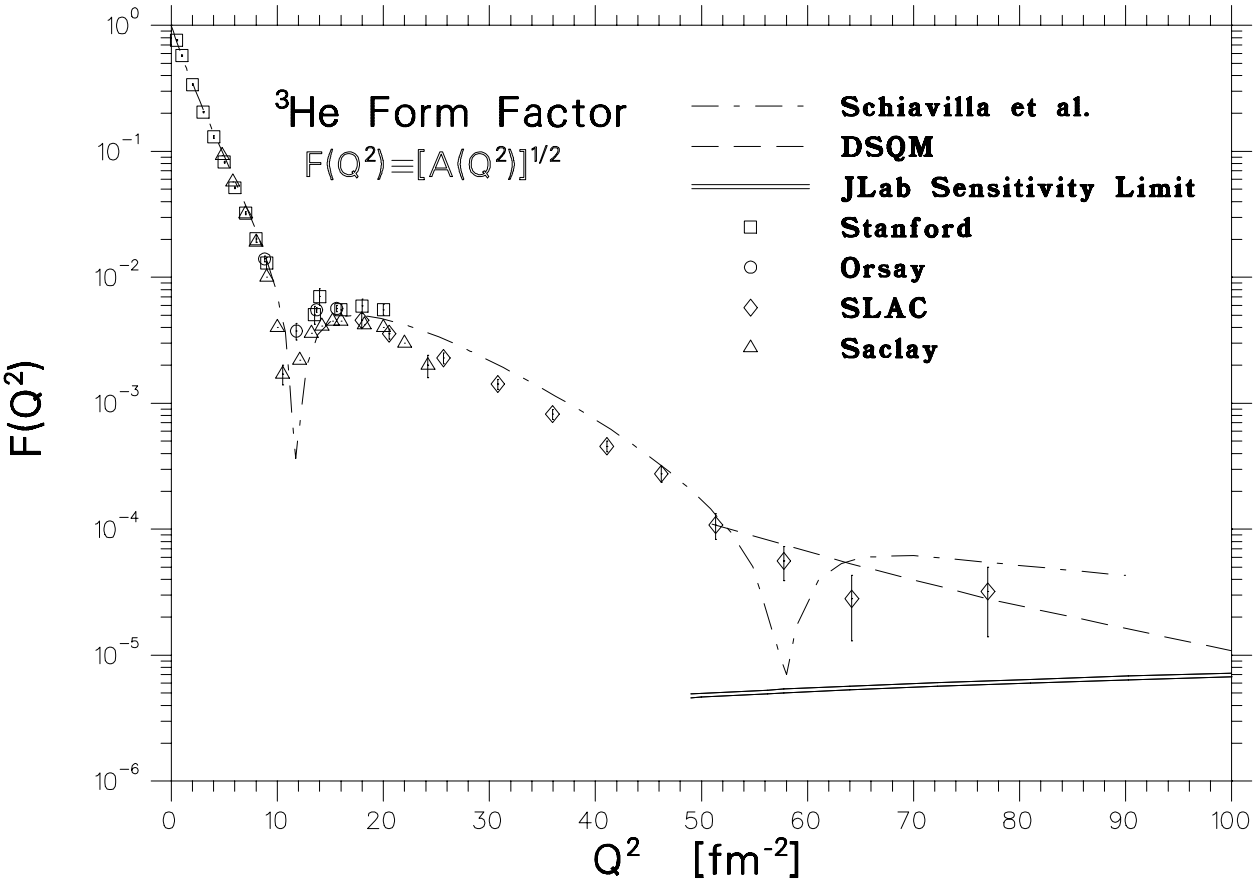


Figure 11: The sensitivity limit ($\sim \pm 30\%$ measurement in a week of beam time at a given $Q^2$) of this experiment for the "$^3$He form factor". Also shown are existing data from Stanford [25, 26], Orsay [27], SLAC [33] and Saclay [29] experiments, and theoretical predictions based on the IA+MEC (Schiavilla *et al.* [8, 9]) and the dimensional-scaling quark model (DSQM, Brodsky and Chertok [24, 40]). The DSQM curve is arbitrarily normalized at $Q^2 = 50$ fm$^{-2}$.

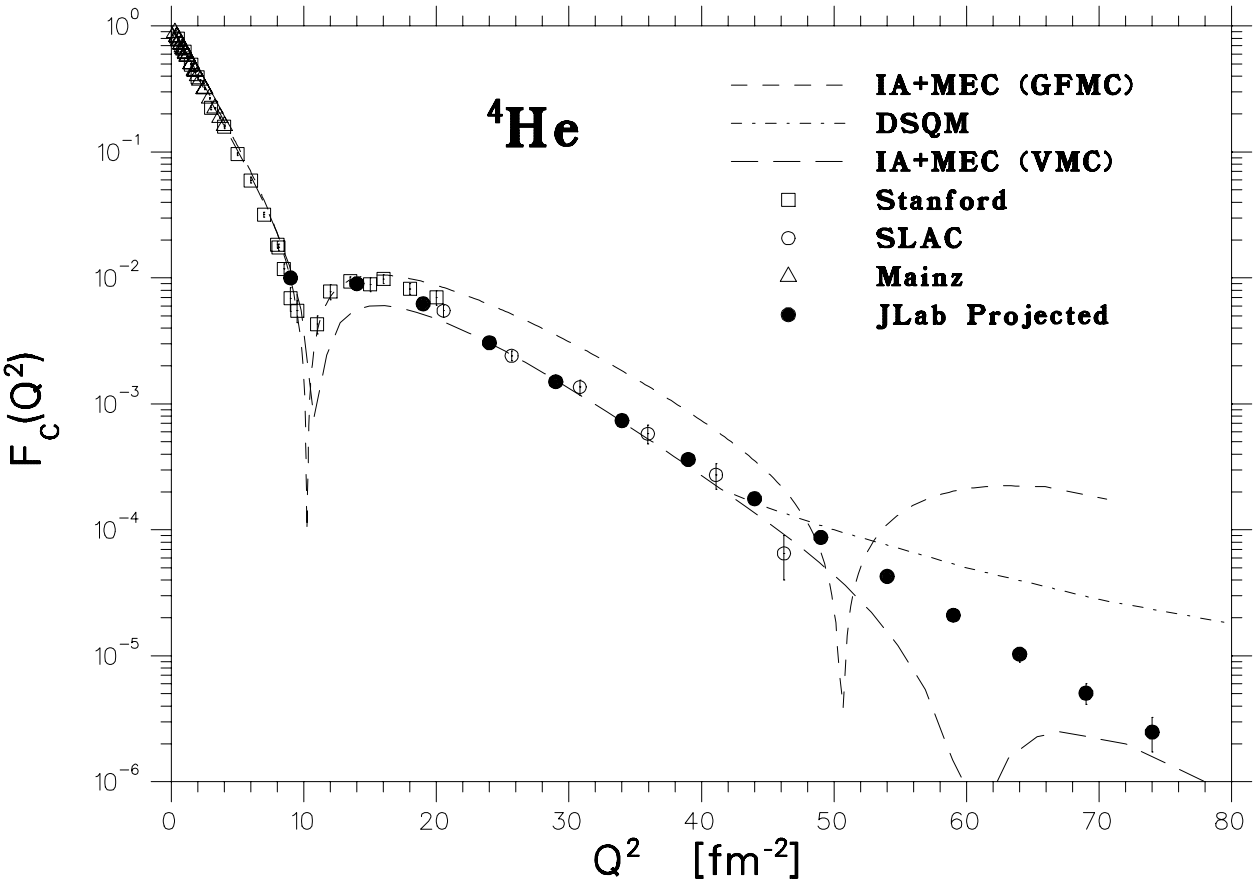


Figure 12: $^4$He charge form factor projected data from this experiment along with the existing Stanford [37, 26], Mainz [32] and SLAC [33] data. Also shown are the variational Monte Carlo (VMC) and Green's Function Monte Carlo (GFMC) calculations by Schiavilla *et al.* [9] and Wiringa [10], and the prediction of the dimensional-scaling quark model (DSQM) of Brodsky and Chertok [24, 40]. The DSQM curve is arbitrarily normalized at $Q^2 = 40$ fm$^{-2}$.